at fixed x and y. Therefore, the solution u^* of Eqs. (7) and (8) forms an upper bound for the solution u of Eqs. (1) and (2) when compared at the same values of x and y.

We cannot solve Eqs. (7) and (8) since ρ^* is unknown, but we can find approximate solutions by replacing ρ^* by ρ_1. These solutions will be called $\bar{u}^*$ and $\bar{w}^*$; they satisfy

$$\bar{u}^* \frac{\partial \bar{u}^*}{\partial x^*} + \bar{w}^* \frac{\partial \bar{u}^*}{\partial y^*} - u_1 u_1'(x) - \nu_1 \frac{\partial^2 \bar{u}^*}{\partial y^{*2}} = 0 \qquad (12)$$

$$(\partial \bar{u}^*/\partial x^*) + (\partial \bar{w}^*/\partial y^*) = 0 \qquad (13)$$

and will be assumed to be known. The relation between $\bar{u}^*$ and u^* is specified in a lemma developed by Nickel,[1] the result of which is as follows. Let $\bar{u}^*$ and u^* be solutions defined in an open region G_1, consisting of $x_1^* < x^* < x_2^*$, $0 < y < \infty$, of the pairs of equations

$$\bar{u}^* \frac{\partial \bar{u}^*}{\partial x^*} + \bar{w}^* \frac{\partial \bar{u}^*}{\partial y^*} - UU'(x^*) - \nu \frac{\partial^2 \bar{u}^*}{\partial y^{*2}} = 0$$

$$\frac{\partial \bar{u}^*}{\partial x^*} + \frac{\partial \bar{w}^*}{\partial y^*} = 0$$

and

$$u^* \frac{\partial u^*}{\partial x^*} + w^* \frac{\partial u^*}{\partial y^*} - UU'(x^*) - \nu \frac{\partial^2 u^*}{\partial y^{*2}} \underset{(\geq)}{\leq} 0$$

$$\frac{\partial u^*}{\partial x^*} + \frac{\partial w^*}{\partial y^*} = 0$$

respectively. If $\bar{u}^*$ and u^* are monotonically increasing functions of y^*, which satisfy the boundary conditions

$$\bar{u}^*(x_1^*, y^*) = u^*(x_1^*, y^*) = \tilde{u}^*(y^*) \qquad \text{for } 0 \leq y^* < \infty$$

$$\bar{u}^*(x^*, 0) = u^*(x^*, 0) = 0 \qquad \text{for } x_1^* \leq x^* < x_2^*$$

and

$$\lim_{y^* \to \infty} \bar{u}^*(x^*, y^*) = \lim_{y^* \to \infty} u^*(x^*, y^*) = U(x^*) \qquad \text{for } x_1^* \leq x^* < x_2^*$$

then

$$u^*(x^*, y^*) \underset{(\geq)}{\leq} \bar{u}^*(x^*, y^*)$$

at fixed values of x^* and y^* everywhere in G.

The problem considered in the present note differs slightly from the one considered by Nickel, in that $u_1(x)$ appears in place of $U(x^*)$, and $\nu_1(x)$ in place of ν. The two variables x and x^* are related by Eq. (4), and Nickel's lemma remains valid when the kinematic viscosity has a specified x^* dependence, so these differences do not affect its conclusion. If we write Eq. (7) as

$$u^* \frac{\partial u^*}{\partial x^*} + w^* \frac{\partial u^*}{\partial y^*} - u_1 u_1'(x) - \nu_1 \frac{\partial^2 u^*}{\partial y^{*2}} = \left(\frac{\rho_1}{\rho^*} - 1\right) u_1 u_1'(x) \qquad (14)$$

we see that, because the temperature profile is monotonic and the external flow velocity is a nondecreasing function of x, the right-hand side of Eq. (14) is never positive. Since $\bar{u}^*$ is the solution of Eq. (14) with the right-hand side replaced by zero, we conclude that

$$u^*(x^*, y^*) \leq \bar{u}^*(x^*, y^*) \qquad (15)$$

by Nickel's lemma. Combining this result with that of Eq. (11), we have

$$u(x, y) \leq \bar{u}^*[x^*(x), y^*(x, y)] \qquad (16)$$

at fixed values of x and y.

The result of the note can be summarized as follows. Say that we have a compressible boundary-layer problem described by Eqs. (1–3) with prescribed boundary conditions on the velocity and with conditions such that the assumptions of monotonic velocity and temperature profiles and the nondecreasing external flow velocity appear reasonable. Then the solution of the related incompressible problem, which has the same x dependent kinematic viscosity and the same boundary conditions on the velocity, gives an upper bound to the velocity profile of the compressible problem.

The result has two immediate generalizations. First, it is reversible in the sense that if the wall is hotter than the external flow we could show that under comparable restrictions the incompressible solution would be a lower bound. Second, the kinematic viscosity can be given an arbitrary known x dependence, such as that described by Stewartson[2] and referred to as the Chapman viscosity law. This can be used to give a more realistic viscosity-temperature relation in the neighborhood of the wall.

References

[1] Nickel, K., "Eine Einfache Abschätzung für Grenzschichten," Ing. Arch. **31**, 85–100 (1962).

[2] Stewartson, K., *The Theory of Laminar Boundary Layers in Compressible Fluids* (Oxford University Press, London, 1964), p. 5.

A New Technique for the Direct Calculation of Blunt-Body Flow Fields

Hsiao C. Kao*
Northrop Corporation, Hawthorne, Calif.

Nomenclature

h = $(1 - V^2)^{1/(\gamma-1)} v$
H = $\rho v^2 + Kp$
g = $\rho u^2 + Kp$
G = $r^j g/R + j(1 + n/R) \cos\theta Kp$
j = 0, 1, two-dimensional problem and axisymmetric problem, respectively
K = $(\gamma - 1)/2\gamma$
p = pressure
s, n = body oriented curvilinear coordinates
t = $(1 - V^2)^{1/(\gamma-1)} u$
u = velocity component in the s direction
v = velocity component in the n direction
V^2 = $u^2 + v^2$
ξ = shock angle
Z = ρuv
γ = ratio of specific heats
δ = shock distance in the n direction
θ = surface angle of the body
ρ = density

Subscripts

0 = condition on the body surface
δ = condition immediately behind the shock wave

Superscripts

$(^-)$ = initial condition on the stagnation axis

All velocities are nondimensionalized by the maximum possible velocity, density by freestream stagnation density, and pressure by freestream stagnation pressure.

Introduction

THE direct integral method for calculating the inviscid hypersonic flow over a blunt body, developed by Belotserkovskii and based on a general numerical method for solving nonlinear hydrodynamic differential equations by

Received July 27, 1964. The author wishes to thank S. A. Powers of Norair for his encouragement and discussion.

* Senior Scientist, Gas Dynamics Branch, Norair Division.

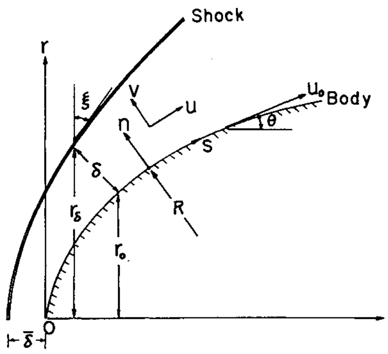

Fig. 1 Coordinate system and flow variables.

Dorodnitsyn, is well known.[1] Although the scheme itself appears to be suitable for machine computation, in practice one encounters a great deal of difficulty in carrying out the numerical integration due to singularities at the sonic line. The nature of these saddle-point singularities has been discussed by previous investigators; for example, Belotserkovskii,[2] Vaglio-Laurin,[3] and Xerikos.[4] The difficulties in approaching these saddle-point singularities render this method almost impractical. The purpose of this note is to show how Belotserkovskii's technique can be modified so that the difficulty of approaching a saddle-point singularity at the sonic line is eliminated. We can, therefore, carry out the numerical integration all the way from the stagnation point (or some other initial point) through the sonic line to the supersonic region.

Governing Equations and Boundary Conditions

The coordinate system and notations used in the following equations essentially follow Refs. 4 and 5. The principal variables used are defined in Fig. 1. The procedure for obtaining the governing equations is as follows:

1) First we express the inviscid equations of continuity, momentum, and energy for a perfect gas in a curvilinear coordinate system with the body as the reference surface.

2) We then recast the governing equations into divergence form by introducing a new set of dependent variables t, h, Z, H, and G (see the Nomenclature) so that we can integrate these partial differential equations along the n direction for each strip.

3) If we assume that r^jt, r^jZ, and G functions can be represented by polynomials in n, we can reduce these integro-differential equations to a set of ordinary differential equations.

For the purpose of illustration, we write these equations of one-strip approximation as follows[1, 4, 5]:

$$\tan(\theta + \xi)(d\delta/ds) - (1 + \delta/R) = 0 \tag{1}$$

$$\begin{aligned}\delta d(r_\delta{}^jZ_\delta)/ds - r_\delta{}^jZ_\delta d\delta/ds + 2r_\delta{}^jH_\delta(1 + \delta/R) - \\ 2r_0{}^jH_0 - \delta(r_\delta{}^jg_\delta + r_0{}^jg_0)/R - \\ jK\delta\cos\theta[p_\delta(1 + \delta/R) + p0] = 0\end{aligned} \tag{2}$$

$$\begin{aligned}(r_0{}^jt_0 - r_\delta{}^jt_\delta)d\delta/ds + \delta[d(r_\delta{}^jt_\delta)/ds + d(r_0{}^jt_0)/ds] + \\ 2r_\delta{}^jh_\delta(1 + \delta/R) = 0\end{aligned} \tag{3}$$

where Eq. (1) expresses a geometrical relation between δ and ξ, and Eqs. (2) and (3) correspond to equations of momentum and continuity, respectively.

To simplify Eqs. (1–3), we usually choose δ, ξ, u_0 as three dependent variables. By making use of the Rankine-Hugoniot relations, we can finally reduce Eqs. (1–3) to Eqs. (4–6), respectively; a form suitable for computation. They are expressed symbolically as follows[4, 5]:

$$d\delta/ds = (1 + \delta/R)\cot(\theta + \xi) \tag{4}$$

$$d\xi/ds = (F_1 + F_2\, d\delta/ds)/F_3 \tag{5}$$

$$du_0/ds = (F_4 + F_5\, d\delta/ds + F_6 d\xi/ds)/F_7 \tag{6}$$

where $F_1 \ldots F_6$ are algebraic functions of δ, ξ, u_0, and θ;

$$F_7 = \delta r_0{}^j(1 - u_0{}^2)^{[(2-\gamma)/(\gamma-1)]} \times [1 - u_0{}^2(\gamma + 1)/(\gamma - 1)]$$

At the sonic point

$$u_0{}^2 = (\gamma - 1)/(\gamma + 1)$$

hence $F_7 = 0$. In order to insure that the surface velocity is not discontinuous at the sonic point on a smooth body, we must let the numerator of Eq. (6) equal zero simultaneously with F_7. Thus, we introduce a singularity at the sonic point (or along the sonic line). This singularity is of the nature of a saddle point. In the numerical computation, we must determine the location of this singularity in order to define the position of the sonic line. Unfortunately, when we perform the numerical integration towards the saddle point with at least one guessed initial condition, the computation is unstable.

Modification and Discussion

If we examine Eqs. (4–6), we find that the saddle-point singularity is mainly due to poor choice of the dependent variables. If we choose δ, ξ, $\eta(= r_0{}^jt_0)$ as three dependent variables, Eqs. (4) and (5) remain essentially the same, but Eq. (6) assumes a different form as follows:

$$d\eta/ds = 2(F_4' + F_5'd\delta/ds + F_6'd\xi/ds)/\delta \tag{7}$$

In addition to the three differential equations (4, 5, and 7) in terms of new dependent variables, we must also have an algebraic equation (8) for evaluating u_0 during the computation:

$$u_0(1 - u_0{}^2)^{1/(\gamma-1)} - t_0 = 0 \tag{8}$$

where $t_0 = \eta/r_0{}^j$. As we can see, the denominator in Eq. (7) is δ, which is the shock distance and which is never zero for any physically realistic problem. Hence, no singularity exists. For higher-order approximations, Eq. (7) is replaced by the equivalent equations whose denominators are the distances of the dividing strips measured from the body surface and are also never zero.

Next we examine the value of t_0 at the sonic point. By differentiating Eq. (8), we can see that t_0 assumes the maximum or minimum values when

$$u_0{}^2 = (\gamma - 1)/(\gamma + 1)(\text{sonic velocity}); \text{ or } u_0{}^2 = 1$$

For a symmetrical body, t_0 varies from zero at the stagnation axis to the maximum value $u_0 = (\gamma - 1)^{1/2}/(\gamma + 1)^{1/2}$ at the sonic point and decreases continuously in the supersonic region. The other root $u_0{}^2 = 1$ corresponds to $t_0 = 0$. A

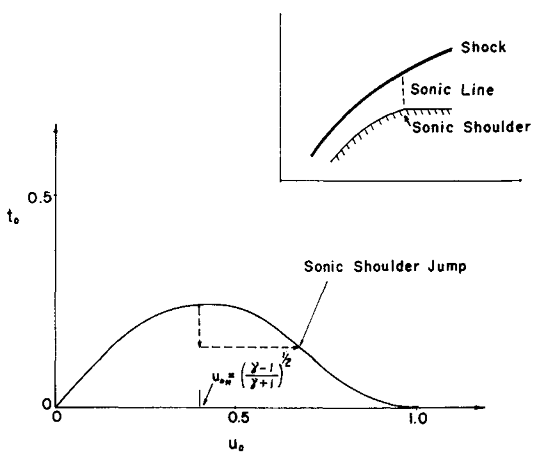

Fig. 2 $u_0 - t_0$ diagram and sonic shoulder jump.

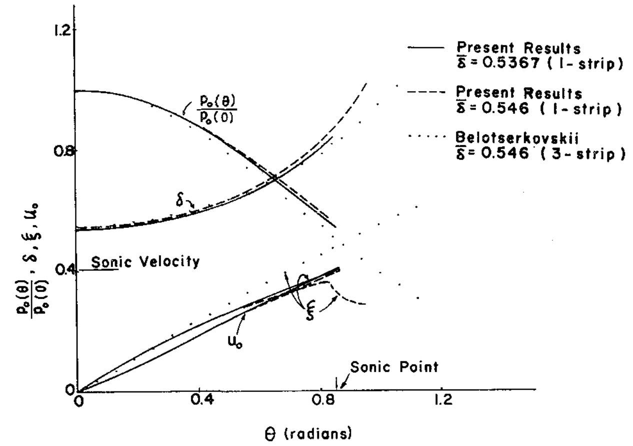

Fig. 3 Numerical results of one-strip approximation for a circular cylinder at $M\infty = 4$, $\gamma = 1.4$ and their comparison with Belotserkovskii's results of two-strip approximation under the same conditions.

schematic plotting of this $u_0 - t_0$ curve is shown in Fig. 2. Thus, for a body with a smooth surface, the sonic point is located where t_0 reaches maximum, or dt_0/ds equals zero. This is in accord with the sonic condition that the acceleration does not become infinite, which is explicitly applied when δ, ξ, and u_0 are used as dependent variables. For a certain class of bodies having sonic shoulders (an example of such a shoulder is shown in Fig. 2), the sonic point is fixed where $u_{0*} = (\gamma - 1)^{1/2}(\gamma + 1)^{1/2}$. After the sonic line the flow undergoes an expansion; u_0 changes from u_{0*} to some higher value within an infinitesimally small distance. Thus, u_0 in the $u_0 - t_0$ diagram jumps abruptly from u_{0*} to $u_0 > u_{0*}$.

To demonstrate the preceding method let us choose a simple example, i.e., a circular cylinder in a supersonic stream with $M_\infty = 4$ and $\gamma = 1.4$ and using a one-strip approximation. The numerical integration is carried out from the stagnation point through the sonic point into the supersonic region. The flow conditions used here are the same as those in Ref. 2, and therefore we can compare the results directly. It should be noted that the results of Ref. 2 are obtained by using a two-strip approximation, whereas ours are the one-strip approximations; hence some discrepancies are to be expected. It is interesting to notice that for an inaccurate guess of the initial condition we can still extend the integration beyond the sonic point without encountering numerical instabilities, though the sonic condition is not satisfied (the dashed-line curves in Fig. 3). With the usual computational scheme, it has been shown in Ref. 4 that, unless the initial condition for one-strip approximation can be guessed to at least six significant figures, the integration diverges before the sonic point is reached. Thus, the advantage of the present scheme is that it is stable near the sonic point.

Although we have only carried out a simple example with one-strip approximations, it is believed that the situation is the same for higher approximations and for more complex geometrical configurations. Work along this line is continuing.

References

[1] Hayes, W. D. and Probstein, R. F., *Hypersonic Flow Theory* (Academic Press, New York, 1959), Chap. VI, p. 202.

[2] Belotserkovskii, O. M., "Calculation of the flow around a circular cylinder with a detached shock wave," Computing Machinery Math., no. 3, 145–185 (1958).

[3] Vaglio-Laurin, R., "On the PLK method and the supersonic blunt-body problem," J. Aerospace Sci. **29**, 185–206 (1962).

[4] Xerikos, J. and Anderson, W. A., "A critical study of the direct blunt-body integral method," Douglas Aircraft Co. Rept. SM-42603 (1962).

[5] Traugott, S. C., "An approximate solution of the direct supersonic blunt-body problem for arbitrary axisymmetric shapes," J. Aerospace Sci. **27**, 361–370 (1960).

Measurements of Errors Caused by Misalignment of Floating-Element Skin-Friction Balances

F. B. O'Donnell* and J. C. Westkaemper†
University of Texas, Austin, Texas

The floating-element skin-friction balance has been used extensively in boundary-layer research. It is probably the most accurate means of measuring skin friction, since it has the advantage of direct measurement, whereas other methods usually involve the deduction of friction forces from temperature or pressure measurements. Experience has shown, however, that special care must be used in testing with the balance in order to realize its theoretical advantages. In particular, the installation requirements include the obvious necessity of aligning the floating element so that it is flush with the test surface. Coles[1] and Dhawan,[2] for instance, both used optical methods to insure the flushness of the element and permitted only a few microinches of misalignment. Other investigators (Smith and Walker[3] and Shutts et al.[4]) concluded that larger misalignments could be tolerated without serious error. It did not appear from these investigations that any systematic study of misalignment effects had been made. Instead, most investigators realized the potential error involved and attempted to minimize the error as much as practicable. Because of the importance of this factor in skin-friction work, an experimental investigation was made to systematically measure the error resulting from misalignment.

Experimental Equipment and Methods

The tests were conducted in a 2- × 2-in. continuous flow wind tunnel. The surface in which the balance was mounted was the flat test-section floor. It was possible to vary the test Mach number by means of an adjustable nozzle, and a Mach Number range of 1.7 to 3.6 was utilized. The flow was adiabatic for all tests.

The operating principles of the balance may be deduced from Fig. 1. The disk-shaped floating element was mounted on a pair of leaf springs which allowed the element to be displaced by the skin-friction forces. The displacement was indicated by a linear variable differential transformer whose output was converted to drag force by means of dead weight calibrations made after each run. The disk diameter was 1 in., and the opening in the tunnel floor was 0.01 in. larger, resulting in an annular gap of 0.005 in. in which the element "floated."

The balance was mounted on a fixed-end support beam (Fig. 2) that restricted the balance motion to translation in a direction perpendicular to the wind-tunnel floor. This beam also served as a restoring spring to return the balance to the recessed position when the displacing force was removed. A drive mechanism was constructed which permitted suitably small increments of balance translation. This mechanism consisted of a differentially threaded lead screw and a cantilever beam. Displacement changes were made by means of a hand wheel attached to the lead screw. As seen in Fig. 2, the lead screw and beam permitted a relatively large rotation of the wheel for small balance translations, thus providing the necessary precision in setting balance misalignments. A correlation between hand-wheel rotation and balance trans-

Received July 27, 1964; revision received September 21, 1964. This work was performed under sponsorship of U. S. Navy Bureau of Weapons, Contract No. NOrd-16498.

* Research Engineer, Defense Research Laboratory; now with Norair Division, Northrop Corporation.

† Research Engineer, Defense Research Laboratory, and Assistant Professor of Aerospace Engineering. Member AIAA.